DOE/ID/12839--T2

CHARACTERIZATION OF OIL AND GAS RESERVOIR HETEROGENEITY

Cooperative Agreement DE-FG07-90ID12839

DOE/ID/12839--T2

DE92 017961

Petroleum Development Laboratory
University of Alaska Fairbanks
437 Duckering Building
Fairbanks, AK 99775-1260

Contract Date: November 1, 1989
Anticipated Completion: March 31, 1993

Principal Investigator:
G. D. Sharma

Project Manager:
Idaho Operations Office

Reporting Period: January 1, 1992 - March 31, 1992

OBJECTIVE

The ultimate objective of this cooperative research project is to characterize Alaskan petroleum reservoirs in terms of their reserves, physical and chemical properties, geologic configuration in relation to lithofacies and structure, and development potential.

The project has two tasks: Task 1 is a geological description of the reservoirs including petrophysical properties, i.e., porosity, permeability, permeability variation, formation depth, temperature, and net pay, facies changes and reservoir structures as drawn from cores, well logs, and other geological data. Task 2 is reservoir fluid characterization—determination of physical properties of reservoir fluids including density, viscosity, phase distributions and composition as well as petrogenesis—source rock identification; and the study of asphaltene precipitation for Alaskan crude oils.

SUMMARY OF TECHNICAL PROGRESS

PETROPHYSICAL AND GEOLOGICAL EVALUATION OF MILNE POINT FIELD

Petrophysical properties of the Milne Point Unit derived from well logs have been tabulated for thirty wells (Table 1). A map of all Milne Point wells is presented in Figure 1. Milne Point wells analyzed to date are shown in Figure 2.

Calculated field-wide average water saturations in Table 1 are higher than those measured within the main producing region of the field (Table 2). Also, field-wide average porosities listed in Table 1 are lower than those taken from wells within the main producing region of the field. Middle Kuparuk production occurs between 6741 ft and 7146 ft subsea. Production from the Lower Kuparuk occurs between 6879 ft and 7525 ft subsea.

Two sandy lobes occurring at the top of each Kuparuk member (four lobes in total) comprise the producing zones in the Upper and Lower Kuparuk. Although production can occur from any of these lobes, it rarely occurs from more than two lobes in any given well. Artificial fracturing of the Lower Kuparuk lobes by the operator (Conoco) has been a common practice in attempting to increase production.

Lower lobes of both the Middle and Lower Kuparuk are not present in several wells, with the Lower Kuparuk exhibiting a greater degree of missing section. Preliminary geologic evaluation indicates that abundant faulting exists within, and adjacent to, the producing areas. Several well logs, including those corresponding to the D-2 well (Figure 3), indicate that a regressive marine environment of deposition may have predominated during Kuparuk (Neocomian) time. Because enough wells have now been analyzed at Milne Point to fully describe the reservoir, complete reservoir description, including placement of faults, structural mapping, stratigraphic analysis, and generation of three-dimensional plots are forthcoming.

Table 1. Field-Wide Log-Derived Petrophysical Properties

ZONE	LOBES	SUBSEA INTERVAL DEPTH (ft)	AVERAGE GROSS THICKNESS (ft)	NET PAY (ft)	AVERAGE POROSITY (%)	AVERAGE WATER SATURATION (%)
Middle Kuparuk	Upper Lobe	-6741 to -7313	17	9	22	66
Middle Kuparuk	Lower Lobe	-6785 to -7146	21[1]	12[1]	25	67
Lower Kuparuk	Upper Lobe	-6879 to -7483	14[2]	6	25	78
Lower Kuparuk	Lower Lobe	-6900 to -7525	23[3]	9	25	79

[1]Present in 47% of wells analyzed.

[2]Present in 87% of wells analyzed.

[3]Present in 70% of wells analyzed.

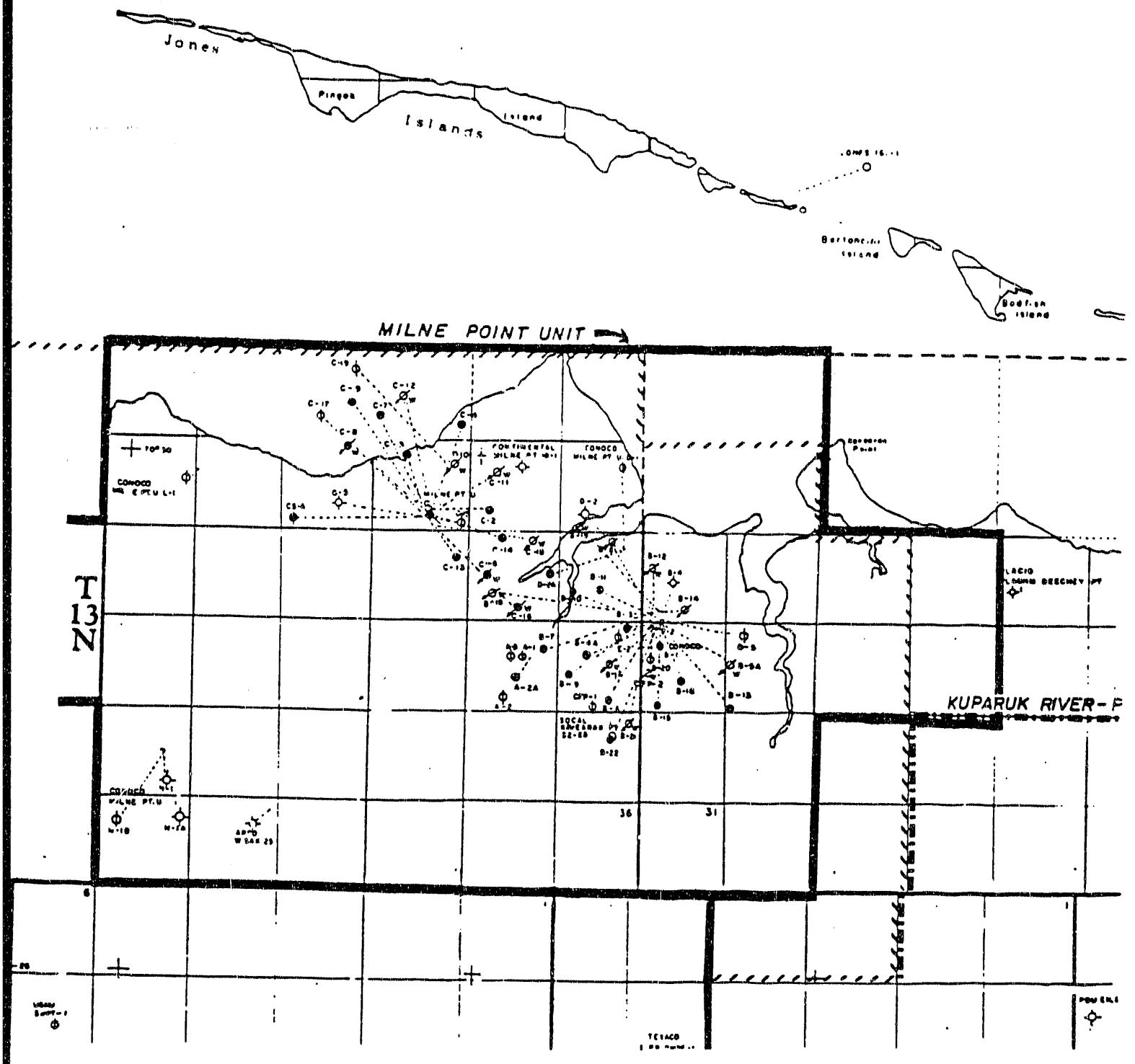

Figure 1. Base Map of Milne Point Wells.

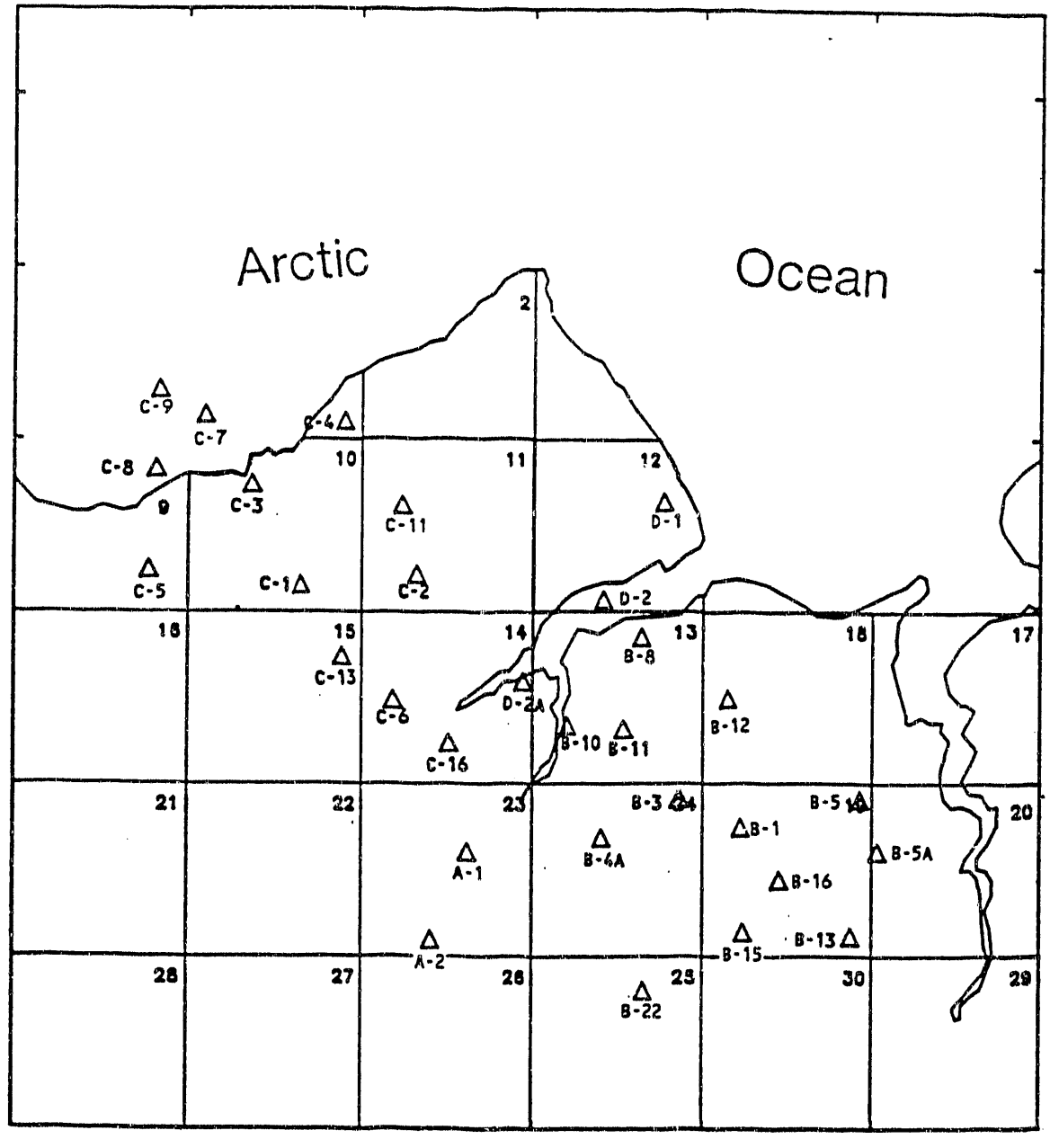

Figure 2. Milne Point Wells Analyzed To Date.

Table 2. Log-Derived Petrophysical Properties
From Wells Within the Center of the Field

ZONE	LOBES	SUBSEA INTERVAL DEPTH (ft)	AVERAGE GROSS THICKNESS (ft)	NET PAY (ft)	AVERAGE POROSITY (%)	AVERAGE WATER SATURATION (%)
Middle Kuparuk	Upper Lobe	-6902 to -6919	17	5	23	43
Middle Kuparuk	Lower Lobe	-6920 to -6940	20	9	27	41
Lower Kuparuk	Upper Lobe	-7086 to -7103	17	3	28	49
Lower Kuparuk	Lower Lobe	-7111 to -7134	23	6	28	46

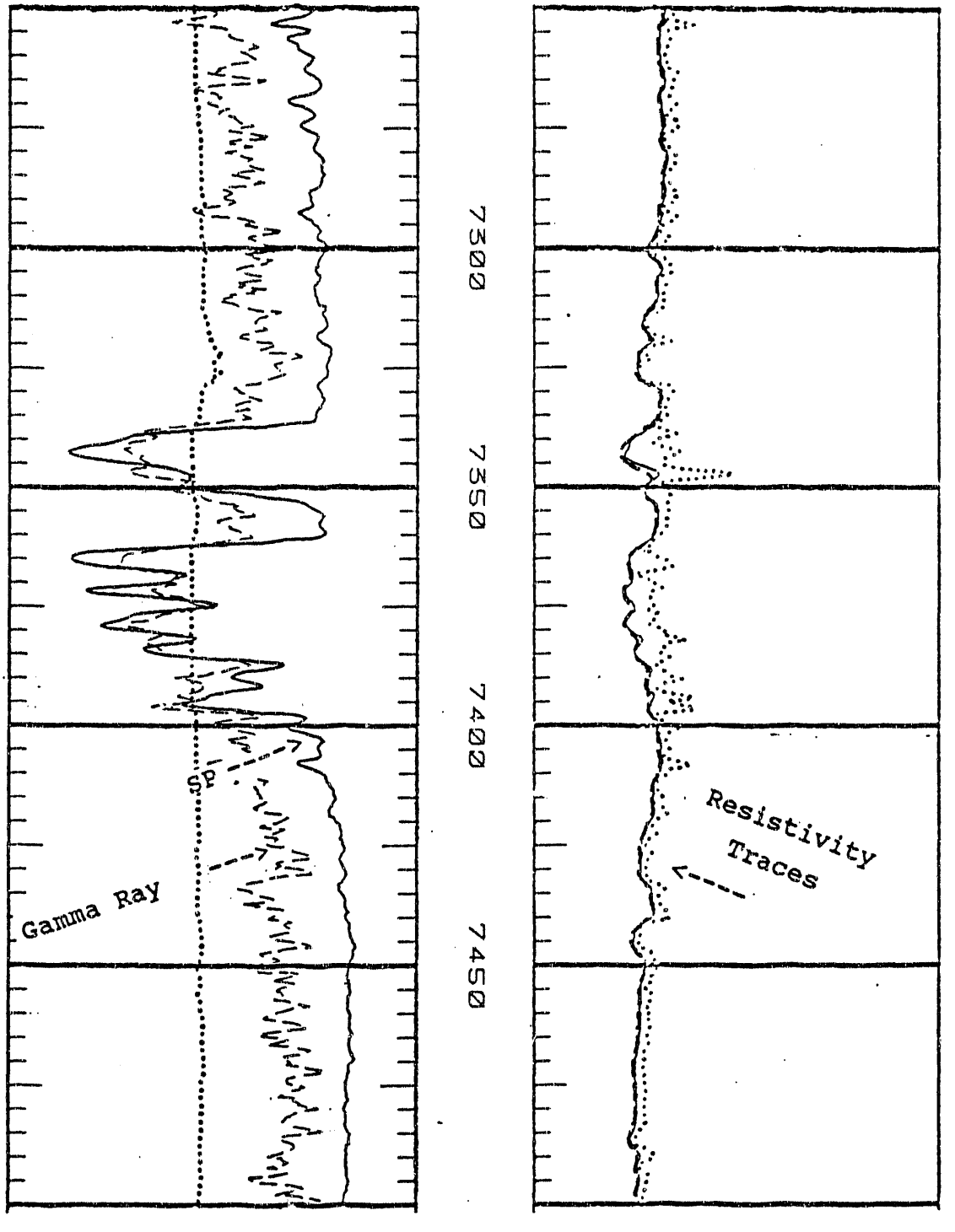

Figure 3. Lower Kuparuk Gamma Ray and SP Traces from Milne Point Well D-2. Trace Character Suggests Regressive Depositional Environment Between 7360' and 7400' (True Vertical Depth).

RESERVOIR FLUID CHARACTERIZATION

Under the reservoir fluid characterization task, work on two subtasks were conducted which include: 1) Modeling of asphaltene equilibria and prediction of asphaltene precipitation from Alaskan crude oils under influence of a miscible solvent; and 2) study of effect of asphaltene deposition on rock-fluid properties. Summary of these studies is provided here.

Modeling of Asphaltene Equilibria and Asphaltene Precipitation

In this work, two approaches have been considered in modeling asphaltene equilibria. In the first approach, a homogeneous molecular thermodynamic model based on Flory-Huggins polymer-solution theory has been developed and coupled with Peng-Robinson equation of state to predict the amount of asphaltene precipitation during injection of enriched gas solvents and CO_2 for the miscible displacement of asphaltic crudes. This model treats asphaltenes within crude oil as a single pseudo-component represented by an average molecular weight, molar volume and solubility parameter. The model was used to predict the amount of asphaltene precipitation during addition of eight different solvents to West Sak crude. The comparison of experimental values of asphaltenes precipitated versus the predicted values is given in Table 3. While the agreement between the predictions and experimental values is excellent, two limitations of the model were realized. First, the model has limited range of applications, since the effect of pressure and temperature on the asphaltene properties such as molar volume and solubility parameter are not incorporated in this model. Second, the treatment of asphaltenes as single component is not appropriate. Thus, this model fails when applied to those solvent-oil systems under wide range of pressures due to variation of molar volume and solubility parameters of liquid phase with pressure and solvent/oil ratio.

Table 3. Comparison of Experimental* and Predicted Amounts of Asphaltene Precipitation for West Sak Tank Oil

*AfterJiang, J.C.etal.

Solvent Used	Solvent/Oil Ratio by Weight	* Wt % Asphaltenes (experimental)	Wt % Asphaltenes (predicted)	% Error
Ethane	3.00	5.14	5.14	0.00
Ethane	13.00	5.28	5.28	0.00
Carbon Dioxide	3.60	5.56	5.50	1.09
Carbon Dioxide	13.60	5.80	6.03	3.97
Carbon Dioxide	15.30	5.89	5.72	2.88
Propane	4.70	8.87	8.34	6.03
Propane	7.80	8.60	9.05	5.02
Propane	16.30	9.07	9.14	0.82
n-Butane	2.00	6.22	6.20	0.34
n-Butane	8.13	6.36	6.43	1.09
n-Butane	13.30	6.45	6.40	0.76
n-Pentane	2.00	6.20	6.47	4.39
n-Pentane	7.00	6.30	5.37	14.78
n_Pentane	12.50	6.69	7.38	10.37
n-Heptane	7.30	5.34	5.41	1.29
n-Heptane	13.50	7.50	8.80	6.06
n-Heptane	20.10	7.32	7.67	4.81
NGL	7.60	8.80	8.80	0.00
NGL	9.90	8.88	8.88	0.00
PBG	1.59	5.49	6.22	13.2
PBG	1.70	7.40	6.24	15.66
PBG	5.85	8.15	7.54	7.54
PBG	10.42	8.08	8.48	5.01

In the second approach, the asphaltenes within crude oil were considered to exist in a wide range of sizes and molecular weights. A polydispersed (heterogeneous) molecular thermodynamic model of asphaltenes has been developed. A normal distribution function has been incorporated to represent various asphaltene fractions having different molecular weights. Twu's (1984) correlation has been incorporated to compute molecular properties of various asphaltene components at different pressures and temperatures based on their molecular weights. The model also incorporates effect of solvent molecular weight through the use of an interaction parameter between asphaltenes and asphaltene-free solvent. Scott-Magat theory has been used to represent asphaltene equilibria and to compute distributions of various asphaltene fractions in the equilibrium liquid and solid phases. The model has also been coupled with Peng-Robinson equation of states to compute effect of solvent/oil ratio and pressure on the asphaltene equilibria represented by solid-liquid equilibrium constant and amount of asphaltene precipitation. The model has been used to predict asphaltene precipitation during addition of eight different solvents to West Sak crude. Table 4 shows the excellent agreement between the experimental results and predicted values. Figure 4 shows the molar distribution of asphaltenes in tank oil, equilibrium solid and liquid phase for n-pentane–West Sak oil. The model has been used to predict asphaltene precipitation from various CO_2–West Sak oil mixtures at various pressures (see Figure 5). The results show that: 1) The higher molecular weight asphaltenes precipitated out while the lower molecular weight asphaltenes remain soluble in the liquid phase. 2) At higher pressures the amount of asphaltene precipitation from CO_2–oil mixtures are considerably lower (0.05-0.2 wt %), but the effect of pressure is complex. 3) The heterogeneous model is more realistic than the homogeneous model in representing asphaltene equilibria.

Table 4. Comparison of Experimental and Predicted Amounts of Asphaltene Precipitation for various Solvents-West Sak Tank Oil Mixtures

SOLVENT	Solvent/Oil Ratio by Weight	Wt. % Asphaltenes experimental	Wt. % Asphaltenes (predicted)	% Error
Ethane	3.00	5.14	5.19	-0.91
Ethane	13.00	5.28	5.22	1.10
Carbon Dioxide	3.60	5.56	5.73	-3.09
Carbon Dioxide	13.60	5.80	5.75	0.88
Carbon Dioxide	15.30	5.89	5.76	2.28
Propane	4.70	8.87	8.88	-0.07
Propane	7.80	8.60	8.88	-3.22
Propane	16.30	9.07	8.88	2.11
N-Butane	2.00	6.22	6.05	2.74
N-Butane	8.13	6.36	6.55	-3.01
N-Butane	13.30	6.45	6.55	-1.56
N-Pentane	2.00	1.79	1.93	-7.69
N-Pentane	7.00	6.20	6.25	-0.65
N-Pentane	12.50	6.30	6.20	1.53
N-Pentane	20.20	6.69	6.20	7.37
N-Heptane	2.00	3.83	3.32	13.31
N-Heptane	7.30	5.34	6.56	-22.76
N-Heptane	13.50	7.50	6.56	12.60
N-Heptane	20.10	7.32	6.56	10.45
NGL	3.20	5.73	5.66	1.16
NGL	7.60	8.80	8.76	0.41
NGL	9.90	8.88	8.78	1.11
PBG	1.59	5.49	4.32	21.24
PBG	1.70	7.40	6.26	15.45
PBG	5.85	8.15	8.12	0.33
PBG	10.42	8.08	8.12	-0.53

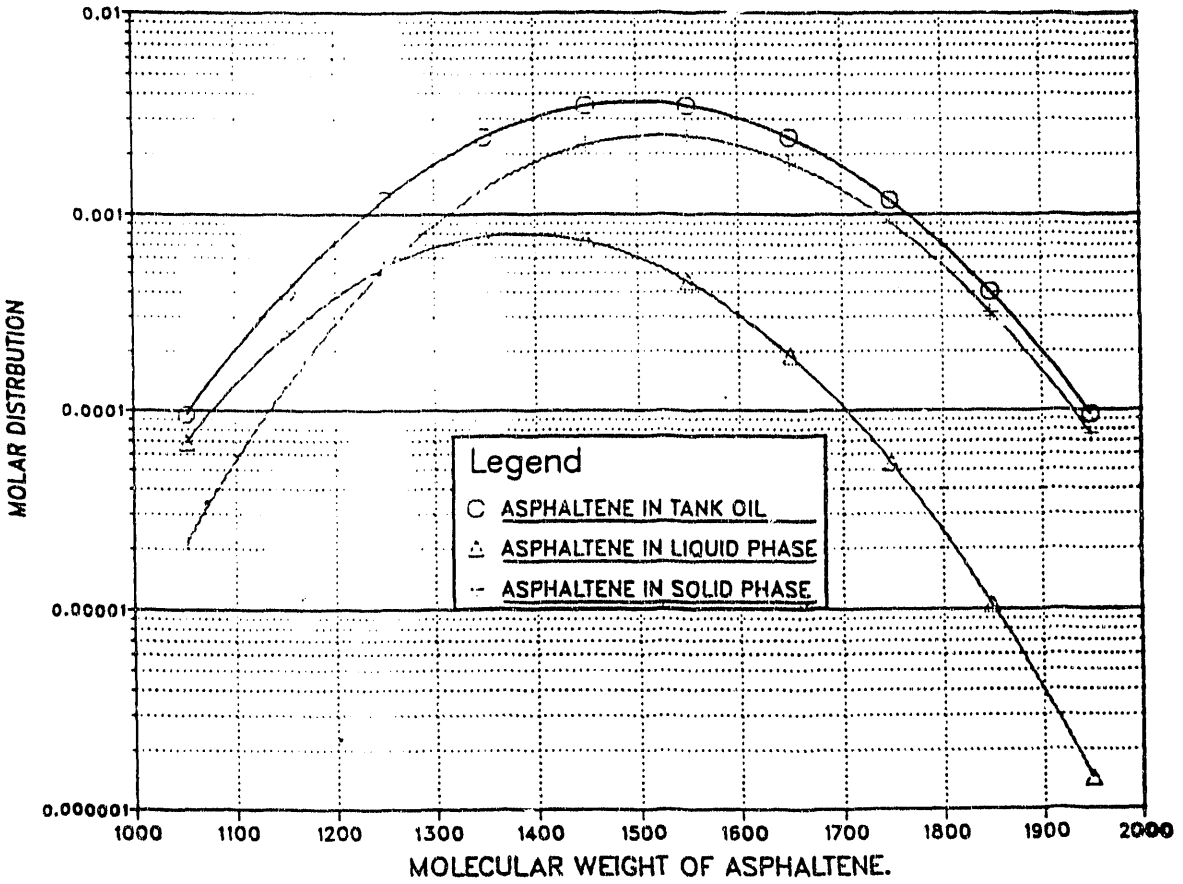

Figure 4. Asphaltenes Mole Fraction Distribution as a Function of its Molecular Weight for n-Pentane-West Sak Tank Oil Solvent/Oil Ratio = 7.0 (By Weight)

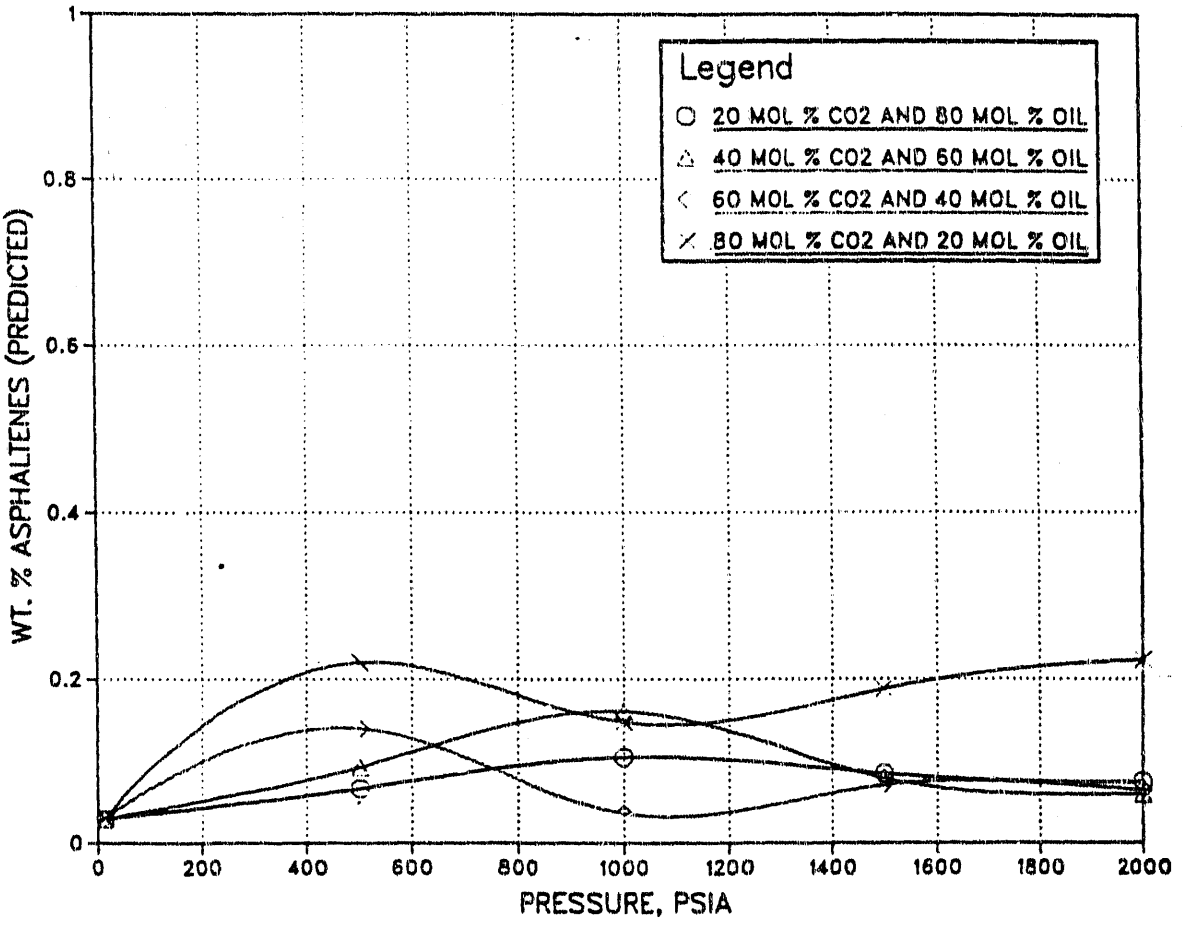

Figure 5. Asphaltenes Precipitation Predictions at different pressures for Carbon Dioxide-West Sak Oil Systems

Effect of Asphaltene Precipitation on Rock-Fluid Properties

The understanding of the effect of asphaltene deposition during miscible displacement processes on the rock-fluid properties is important since the asphaltene deposition will affect the sweep and displacement efficiencies of such processes. Previous work reported in literature shows that asphaltene deposition changes the rock wettability from water-wet to oil-wet, but no studies have been reported on the effect of asphaltene deposition on the absolute permeability and relative permeability curves.

In this work, so far four experiments have been conducted using 1-inch diameter, 12-inch long Berea sandstone core to determine the effect of asphaltene precipitation on absolute permeability and relative permeability curves. Figure 6 shows the schematic diagram of the experimental setup constructed for this study. Figure 7 shows the effect of amount of asphaltene precipitation on the absolute permeability of the core. These results show that asphaltene precipitation reduces the absolute permeability of the core by about 50% for this core. Figure 8 shows the effect of pore volumes of water injected on the displacement efficiency for all four runs. The results show that the displacement efficiency is improved by asphaltene deposition. This may be due to the fact that although asphaltene deposition reduces the absolute permeability, the relative oil permeability is improved due to wettability alteration by asphaltene deposition. Further work is in progress to conduct experiments for two additional types of porous media. It is expected that the pore size distribution, the average pore size, and the initial permeability of the porous media will also play a role in the effect of asphaltene deposition on rock-fluid properties.

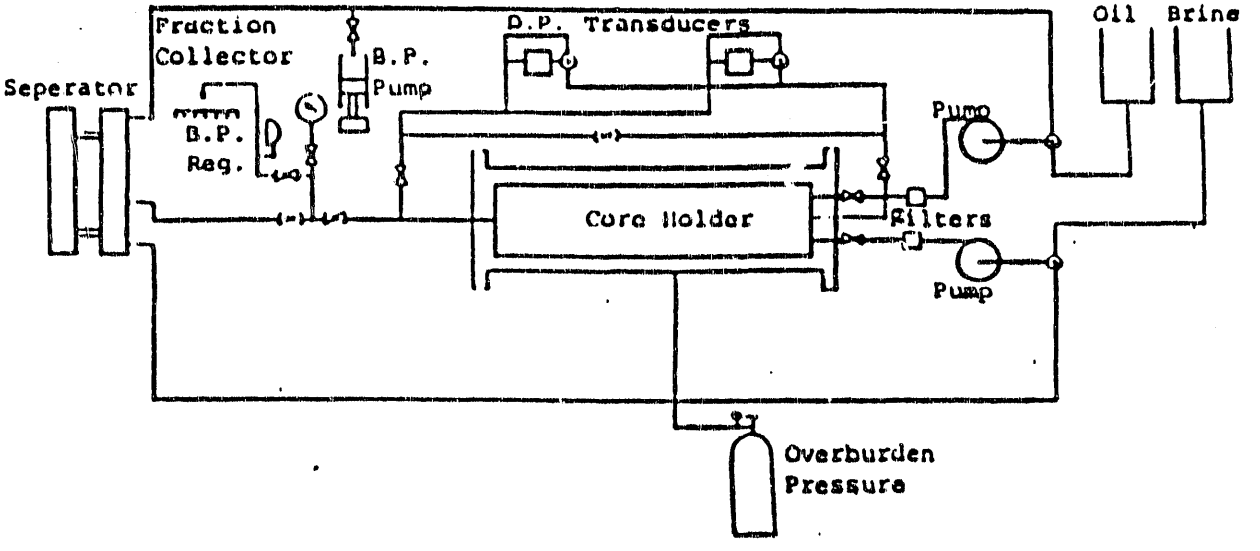

Figure 6. Schematic Diagram of Experimental Setup

Fig.7: Effect of wt% asphaltene Deposited on the Ratio of Absolute Permeability after deposition To Initial Absolute Permeability

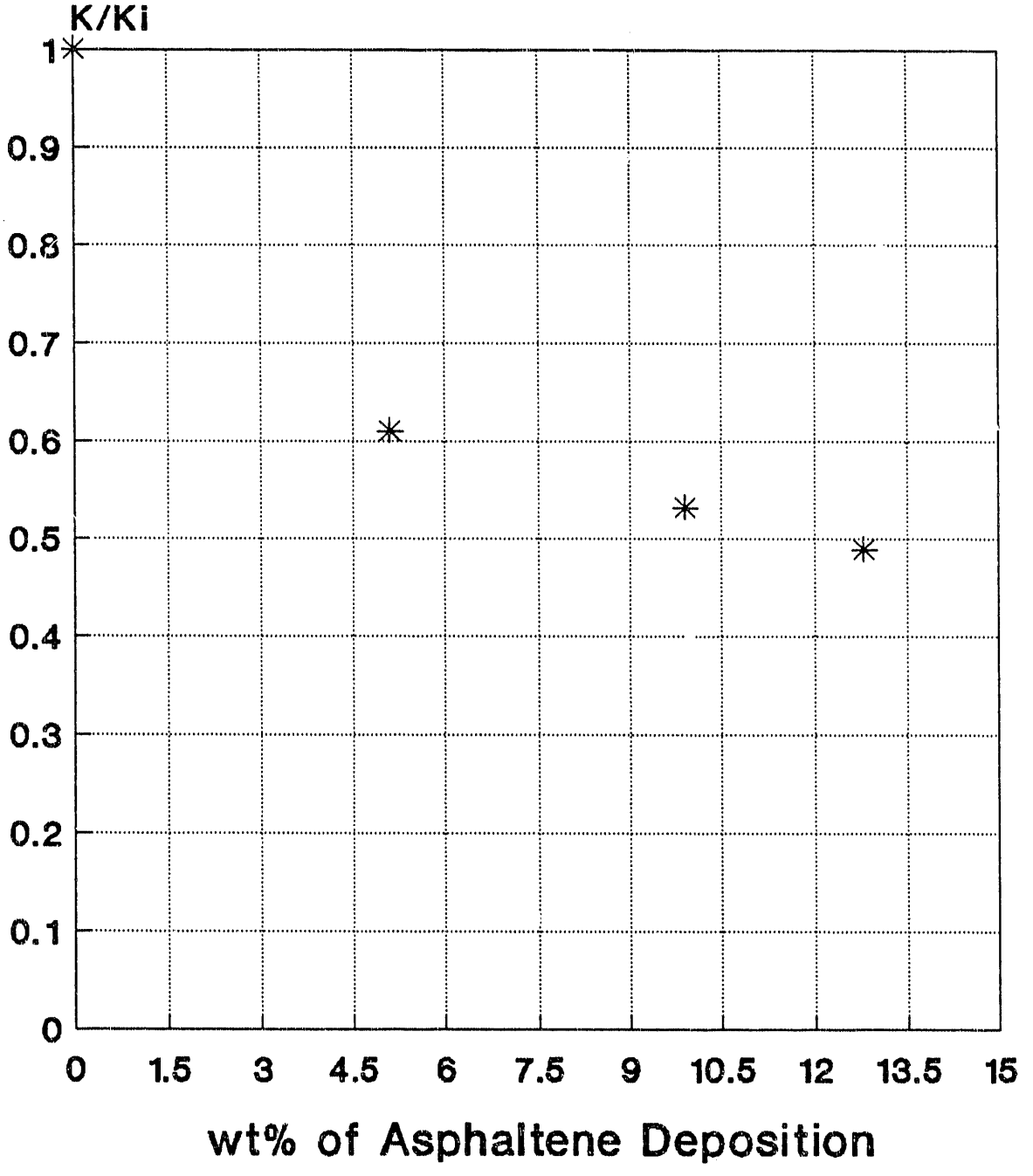

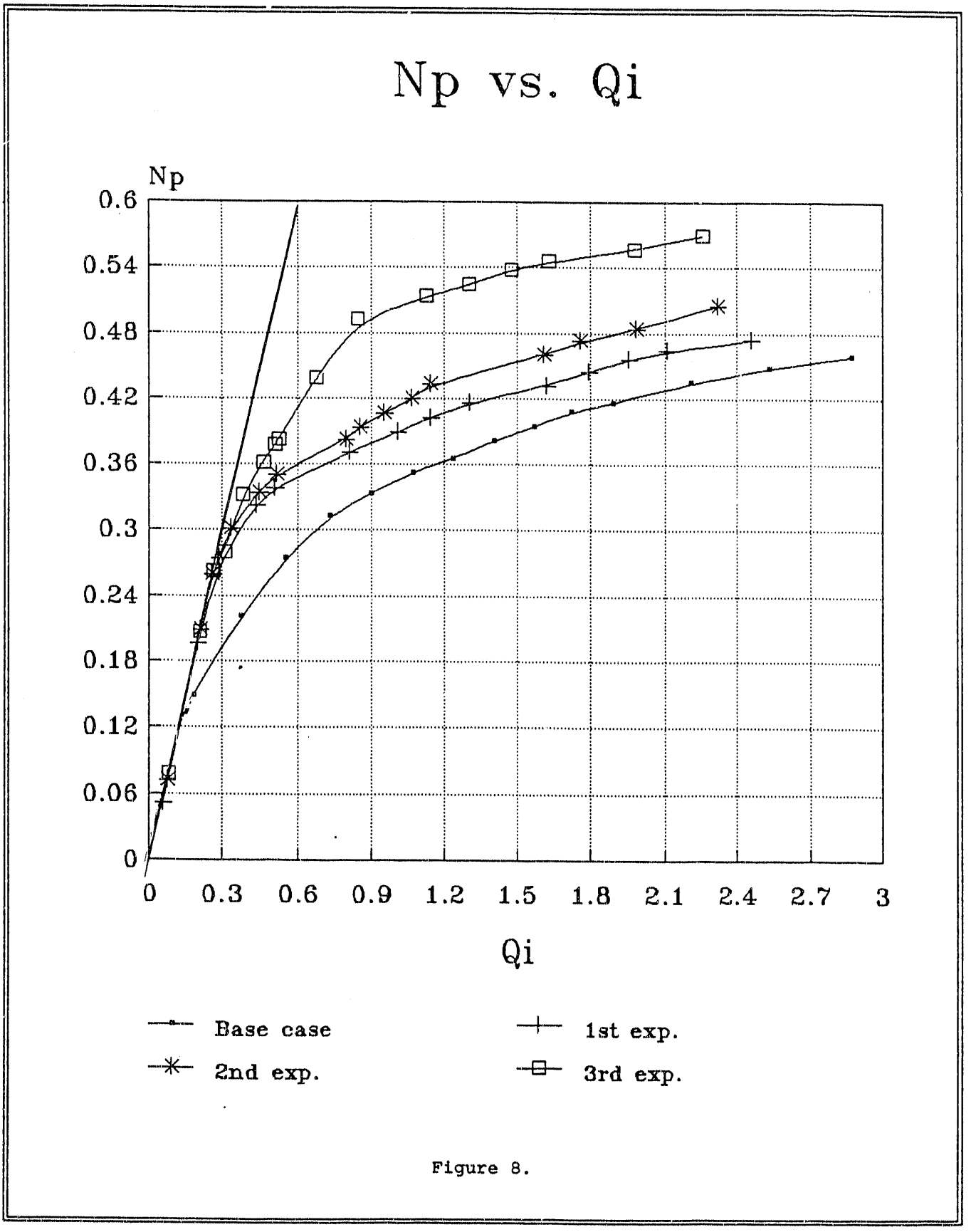
Np vs. Qi
Np
0.6
0.54
0.48
0.42
0.36
0.3
0.24
0.18
0.12
0.06
0
0
0.3
0.6
0.9
1.2
1.5
1.8
2.1
2.4
2.7
3
Qi
Base case
1st exp.
2nd exp.
3rd exp.

Figure 8.

REFERENCES

1. Jiang, J.C., S.L. Patil, and V.A. Kamath: *"Study of Asphalt/Asphaltene Precipitation During Addition of Solvents to West Sak Crude,"* ACS Petroleum Chemistry Division Symposium on Chemistry and Characterization of Asphalt, Vol. 35, No. 3 (July 1990), pp. 522-530.

2. Twu, C.H.: *"An Internally Consistent Correlation for Predicting Critical Properties and Molecular Weight of Petroleum and Coal Tar Liquids,"* Fluid Phase Equilibria, Vol. 16, No. 2 (1984), pp. 137-150.

END

DATE
FILMED
9/01/92